


 Cite this: *RSC Adv.*, 2021, 11, 37150

# Surface coating of a $\text{LiNi}_x\text{Co}_y\text{Al}_{1-x-y}\text{O}_2$ ( $x > 0.85$ ) cathode with $\text{Li}_3\text{PO}_4$ for applying a water-based hybrid polymer binder during Li-ion battery preparation†

 Tatsuya Watanabe,<sup>a</sup> Tamae Yokokawa,<sup>a</sup> Mitsuru Yamada,<sup>a</sup> Shoudai Kurosumi,<sup>b</sup> Shinsaku Ugawa,<sup>b</sup> Hojin Lee,<sup>b</sup> Yuta Irii,<sup>c</sup> Fumihiko Maki,<sup>c</sup> Takao Gunji,<sup>d</sup> Jianfei Wu<sup>d</sup> and Futoshi Matsumoto<sup>\*,a</sup>

To produce water-stable Ni-rich lithium nickel cobalt aluminum oxides ( $\text{LiNi}_x\text{Co}_y\text{Al}_{1-x-y}\text{O}_2$ ,  $x > 0.85$ , NCAs), the formation of trillithium phosphate ( $\text{Li}_3\text{PO}_4$ )-coated layers on the NCA surfaces was attempted through the use of a surface reaction in a mixture of ethanol and water and a post-heat treatment at 350 and 400 °C. Based on the results of X-ray photoelectron spectroscopy (XPS), the coated layers consisted of nickel phosphate ( $\text{Ni}_3(\text{PO}_4)_2$ ) and  $\text{Li}_3\text{PO}_4$ . The coated NCA surface could have sufficient water stability to maintain the cathode performance in a water slurry for 1 day. In addition, the coated layers formed on the NCA surfaces did not block  $\text{Li}^+$ -ion transfer through the  $\text{Ni}_3(\text{PO}_4)_2/\text{Li}_3\text{PO}_4$ -coating layers and enhanced the high-rate discharge performance.

 Received 24th August 2021  
Accepted 20th October 2021

DOI: 10.1039/d1ra06409f

[rsc.li/rsc-advances](https://rsc.li/rsc-advances)

## 1 Introduction

Lithium-ion batteries (LIBs) have spread to our daily life as power sources of mobile devices<sup>1,2</sup> and are helping to establish the world of electrically driven vehicles.<sup>3,4</sup> LIBs are chemical devices in which chemical energy converts to electrical energy in the discharging process and electrical energy converts to chemical energy in the charging process.<sup>5,6</sup> The chemicals bear the energy conversion in the LIB. Chemicals such as anodes, cathodes, electrolytes, solvents, binders, and conductive additives have been designed for them to not only exhibit maximum performance but also to not cause trouble for other chemicals.<sup>7-9</sup> Usually, electrolytes, solvents, binders, conductive additives and so on have also been modified for anode and cathode materials to exhibit maximum performance.<sup>10,11</sup> Moreover, recently, in anode and cathode materials, their composition and surface had to be modified to increase the battery performance and to decrease the cost of LIBs.<sup>12-14</sup> For example, coating the cathode surface was attempted to prepare a cathode

with a water-based slurry.<sup>15,16</sup> Aqueous processes for the fabrication of anode and cathode electrodes in LIBs with water-soluble and aqueous polymers, *i.e.*, water-based polymers, have attracted much attention as binders to establish environmentally compatible fabrication processes for LIBs and to reduce the price of LIBs.<sup>17,18</sup> In the conventional slurry process, poly(vinylidene difluoride) (PVdF) polymer binder, active materials and conductive additives are dissolved in *N*-methylpyrrolidone (NMP) solvent, which is listed as a carcinogenic chemical with reproductive toxicity and should be collected without atmospheric emission.<sup>19</sup> Then, the slurry is cast on current collectors, and finally, the solvent is evaporated in a vacuum drying process to form an active material layer on the current collector. The cathode materials dissolved increasingly less in water and the charging/discharging cycle performance was degraded when the surface was in contact with water.

Ni-rich lithium nickel cobalt aluminum oxide ( $\text{LiNi}_x\text{Co}_y\text{Al}_{1-x-y}\text{O}_2$ , NCA) cathode materials, which are responsible for the energy storage capability of Panasonic cylindrical 18650 cells, exhibit a higher reversible capacity ( $>190 \text{ mA h g}^{-1}$ ) and are regarded as an attractive cathode material due to their outstanding electrochemical performance, thermal stability and environmentally friendly features.<sup>20-22</sup> However, NCAs still have several problems, such as severe capacity fading during the charge-discharge process and thermal runaway attributed to structural instability.<sup>23,24</sup> In addition, there are serious problems with the dissolution of the surface of NCAs and the lithium ion/proton ( $\text{Li}^+/\text{H}^+$ ) exchange reaction from/into NCAs caused by contacting the NCA surfaces with water and then a drastic drop

<sup>a</sup>Department of Materials and Life Chemistry, Kanagawa University, 3-27-1, Rokkakubashi, Kanagawa-ku, Yokohama, Kanagawa 221-8686, Japan. E-mail: [fmatsumoto@kanagawa-u.ac.jp](mailto:fmatsumoto@kanagawa-u.ac.jp)

<sup>b</sup>JSR Corporation, 100 Kawajiri-cho, Yokkaichi, Mie 510-8552, Japan

<sup>c</sup>Nihon Kagaku Sangyo Co., Ltd., 1-28-13 Nakane, Soka, Saitama 340-0005, Japan

<sup>d</sup>Qingdao Industrial Energy Storage Research Institute, Qingdao Institute of Bioenergy and Bioprocess Technology, Chinese Academy of Sciences, No. 189, Songling Road, 266101 Qingdao, China

† Electronic supplementary information (ESI) available. See DOI: 10.1039/d1ra06409f



in the charging/discharging capacities.<sup>25–29</sup> For NCAs to avoid water contact, various surface coatings of NCAs were proposed<sup>15,30,31</sup> as well as the addition of acid and buffer chemicals to keep the pH in aqueous slurry.<sup>32–34</sup> Trilithium phosphate ( $\text{Li}_3\text{PO}_4$ ) coating on NCAs to give waterproof properties to the surface of NCAs has been attracted.<sup>35,36</sup> The  $\text{Li}_3\text{PO}_4$  surface layer is also applied to conventional LIBs in which cathodes are prepared with a conventional solvent process with a PVdF binder and NMP solvent to hinder side reactions between the cathode and the organic electrolyte and oxygen release from the cathode surface, resulting in the improvement of cathode performance and thermal stability.<sup>37–40</sup>  $\text{Li}_3\text{PO}_4$  has chemical and thermal stability and exhibits intrinsic  $\text{Li}^+$  conductivity with stable  $\text{P}=\text{O}$  bonds.<sup>37–40</sup> Wet coating of  $\text{Li}_3\text{PO}_4$  is a simple method by adding phosphate ion ( $\text{PO}_4^{3-}$ ) ions to a reaction solution in which NCA particles are dispersed. On the NCA surface,  $\text{PO}_4^{3-}$  ions react with lithium hydroxide ( $\text{LiOH}$ ) and lithium carbonate ( $\text{Li}_2\text{CO}_3$ ) residues formed on the NCA surface, and then  $\text{Li}_3\text{PO}_4$  is formed on the NCA surfaces. As mentioned above, there are several reports that  $\text{Li}_3\text{PO}_4$ -coated NCA has waterproof properties and that NCA cathodes prepared with aqueous processes exhibit more stable cathode performance than those prepared with conventional organic solvent processes.<sup>35,36</sup> However, we cannot think that  $\text{Li}_3\text{PO}_4$ -coated NCA has water-proof properties enough to apply  $\text{Li}_3\text{PO}_4$ -coated NCA to commercially available LIB production because the results were obtained with cathodes prepared with fresh slurry and  $\text{Li}_3\text{PO}_4$ -coated NCA was not exposed for a long time. When slurry solutions of electrode active materials are used, once prepared, typically for one day at least in the production line of commercially available LIBs. Therefore, the slurry that was stored for a long time should be used to prepare the cathodes for performance testing of  $\text{Li}_3\text{PO}_4$ -coated NCA.

Additionally, in this study, a  $\text{Li}_3\text{PO}_4$  coating on NCA particle surfaces was examined because of the simple wetting process of the  $\text{Li}_3\text{PO}_4$  layer and the suitable property of  $\text{Li}_3\text{PO}_4$  as a protective layer. In contrast to other research, a mixture of water and ethanol was used as a solvent for the coating process. Giffin *et al.* used ethanol as the solvent for the coating process.<sup>35,36</sup> We think that they considered the employment of ethanol solvent in the coating process to lower the acidity of  $\text{H}_3\text{PO}_4$  and inhibit the dissolution of Li and nickel (Ni) ions from the NCA particle surfaces. However, we think that the reaction of eqn (1) hardly occurs in ethanol solvent.



To accelerate the reaction of eqn (1), water might be needed. Therefore, we used a mixture of water and ethanol as a solvent for the coating process. Although the results are not shown in this paper, we examined the ratio of water/ethanol for the coating solvent and the concentration of phosphoric acid ( $\text{H}_3\text{PO}_4$ ) as a source of  $\text{PO}_4^{3-}$  ions added to the coating solution. In addition, the  $\text{Li}_3\text{PO}_4$ -coated NCA cathodes were prepared with aqueous slurries stored for 1 and 24 h after the preparation of the slurries.  $\text{Li}_3\text{PO}_4$  is water-soluble. Therefore, the  $\text{Li}_3\text{PO}_4$

layer formed on the NCA surface will be dissolved from the NCA surface to aqueous slurry during the storage of the slurries. To overcome this problem, the  $\text{Li}_3\text{PO}_4$ -coated NCA samples were thermally treated (heat-treated) at temperatures from 200 to 450 °C to form water-insoluble layers in the reaction between the coated  $\text{Li}_3\text{PO}_4$  and the NCA surface.

## 2 Experimental

$\text{LiNi}_a\text{Co}_b\text{Al}_{1-a-b}\text{O}_2$  ( $a > 0.85$ ) particle sample (NCA, cat. # NC-02, Nihon Kagaku Sangyo Co., Ltd., Japan) was used as an NCA cathode material for  $\text{Li}_3\text{PO}_4$  coating. Particles with  $D_{50\%} = 14 \mu\text{m}$  were used without any purification. Surface coating with  $\text{Li}_3\text{PO}_4$  was conducted using a wet method, as shown in Fig. S1.† Four grams of NCA particles was dispersed in ethanol (10 g) with a magnetic stirrer at 25 °C for 2 min. Then, 0.05 M  $\text{H}_3\text{PO}_4$  aqueous solution (2.4 mL) was dropped to the NCA-dispersed ethanol solution for 10 min. After dropping the  $\text{H}_3\text{PO}_4$  solution, the mixture of water, ethanol and NCA particles was stirred at 25 °C for 30 min. After filtration of the resulting NCA particle, the particles were dried up at 130 °C for 1 h and then sintered at 200–450 °C for 2 h in an argon (Ar) or air atmosphere to form the coating layer on the NCA particle surface. The coated NCA particles were characterized with scanning electron microscopy (SEM), powder X-ray diffraction (pXRD), X-ray photoelectron spectroscopy (XPS) and scanning transmission electron microscopy-X-ray energy-dispersive spectrometry (STEM-EDX). Their equipment and measurement conditions are described in the experimental section of ESI.† For the water stability test of the coated NCA particles, 1 g of coated particles was dispersed in 5 mL of water for 1 h. After 1 h, the coated NCA particles were dried at 130 °C for 1 h, and their surfaces were observed with SEM to confirm the water stability of the coated NCA particles.

The methods for cathode preparation and cathode performance testing with coated and pristine NCA are also described in the experimental section of ESI.† Cathodes were prepared with coated and pristine NCA in the water process with aqueous slurry in which NCA, water-based hybrid polymer binder TRD202A (JSR, Japan), carboxymethyl cellulose (CMC) and conductive additive (acetylene black (AB)) were dispersed in water. The prepared aqueous slurries were left for 1 and 24 h before casting on aluminum (Al) current collector foil to confirm the stability of NCA against water. The pH of the slurries was measured with a pH meter at 30, 60 and 90 min after slurry preparation. The concentration of Ni ions in slurries, which were dissolved from NCA surfaces to the slurry solutions, was analyzed with inductively coupled plasma-mass spectrometry (ICP-MS, Agilent, 7700× spectrometer).

In charging/discharging cycle and C-rate performance tests of coated NCA cathodes, constant-current/constant-voltage (CC-CV) mode was applied to NCA cathodes. The cutoff voltage and charge/discharge current density were 2.5–4.25 V (vs.  $\text{Li}/\text{Li}^+$ ) and 0.1–5 C, respectively. The pristine NCA cathode prepared with PVdF binder exhibited a discharge capacity of 200 mA h  $\text{g}^{-1}$ . In the calculation of the discharge capacity retention, 200 mA h  $\text{g}^{-1}$  was considered an indicator of 100% capacity retention.

### 3 Results and discussion

#### 3.1 Characterization of coated NCA cathode materials

Fig. 1 shows the SEM images of (a) pristine NCA particles, (b–g) coated NCA particles without (b) and with (c–h) heat treatment at (c) 200, (d) 250, (e) 300, (f) 350, (g) 400 and (h) 450 °C under (A) Ar and (B) air atmospheres. Usually, the heat treatment under Ar atmosphere is applied to the samples to form coated layer of  $\text{Li}_3\text{PO}_4$  having high degree of crystallinity. In this study, the heat treatment under air atmosphere was examined because compounds other than  $\text{Li}_3\text{PO}_4$  should be produced and the compounds protect efficiently the surface of NCA particles. The surfaces (b–h) of NCA particles on which the  $\text{Li}_3\text{PO}_4$  moiety is covered are rougher than those of uncoated NCA (a). Moreover, the surface of coated NCA particles (c–h) after heat treatment became rougher than that of coated NCA particles (b) without heat treatment due to an increase in the degree of crystallinity of  $\text{Li}_3\text{PO}_4$  by heat treatment. The difference in the surface morphology between the coated NCA particles heat-treated under Ar and air cannot be observed from the SEM images in Fig. 1.

The coated layers formed on the NCA particle that was heat-treated at 400 °C under air were observed with TEM (Fig. 2) and TEM-EDX (Fig. 3). Before the heat treatment, the coated layer was thick, and its thickness was 50–100 nm (Fig. 2(a)). The coated layer shrank after the heat-treatment. In the case of heat treatment under an Ar atmosphere, the thickness of the coated layer became 20–30 nm. Under an air atmosphere in the heat treatment, the coated layer shrank more, and its thickness was 10–20 nm. From the TEM-EDX images of the coated layers after heat treatment (Fig. 3), it was confirmed that the NCA surfaces were covered uniformly with the coated layers containing phosphorus atoms. The thickness of the coated layers after heat treatment decreased with the increase in temperature for heat treatment, resulting in a higher density of the coated layer with an increase in the temperature of heat treatment. The decrease in the thickness of the coated layers after the heat treatment under Ar and air might be due to shrinkage, resulting in an increase in the density of the coated layer, or decomposition of the coated layer for the decomposition products to fly from the coated layer along Ar and air flows. In addition, when compared

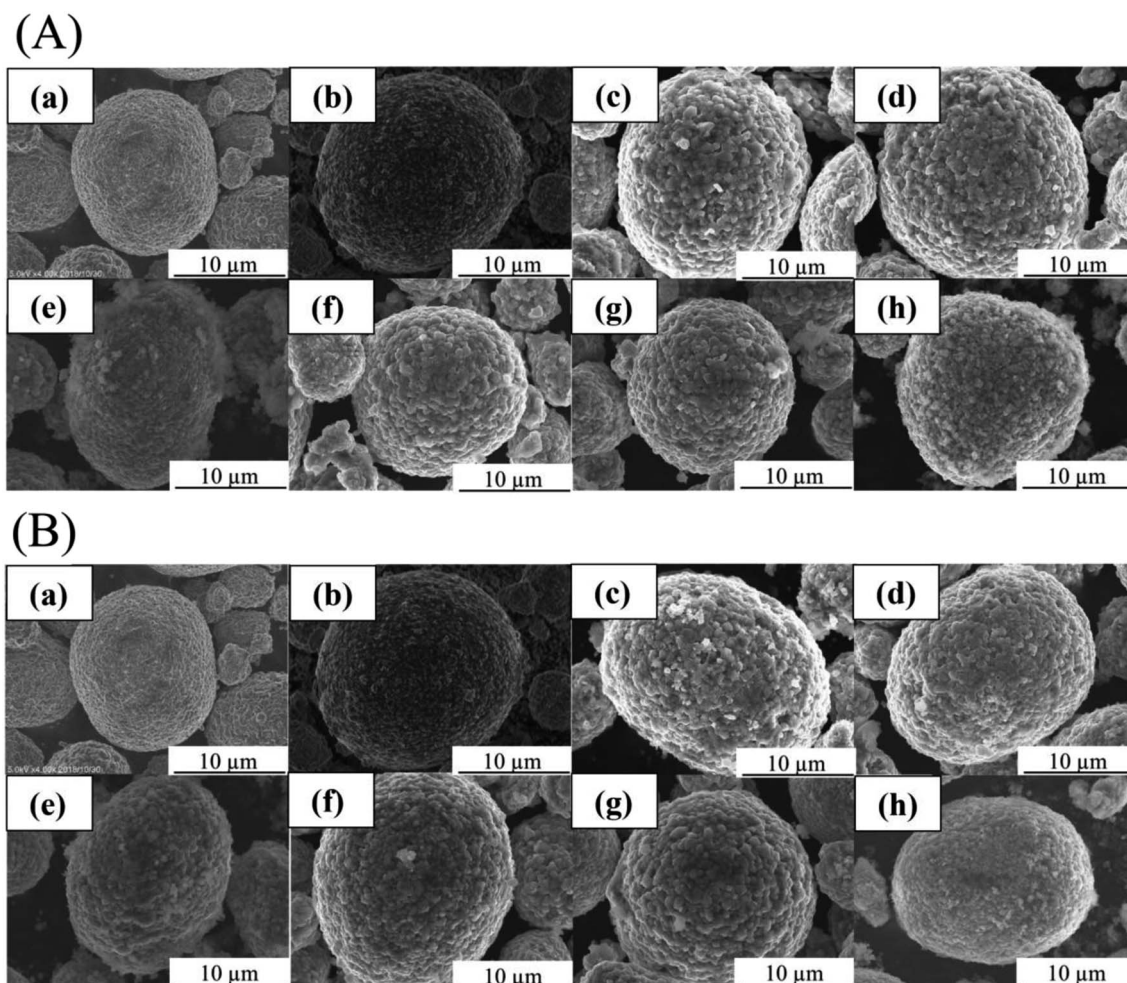


Fig. 1 SEM images of (a) pristine NCA and (b–h) coated NCA samples. (b) Coated NCA samples without heat treatment, (c–h) coated NCA with heat treatment. Temperature of heat treatment: (c) 200, (d) 250, (e) 300, (f) 350, (g) 400 and (h) 450 °C. Atmosphere for heat-treatment: (A) Ar and (B) air.

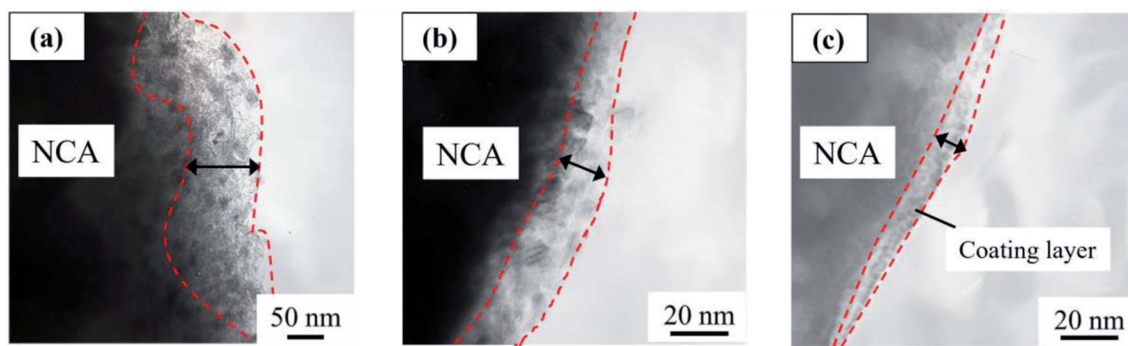


Fig. 2 TEM images of coated NCA (a) without heat treatment and with heat treatment at 400 °C in (b) Ar and (c) air atmospheres.

between EDX images of Ni and Co, Ni atoms distribute more widely than Co. Fig. S2† shows TG-DTA charts of (a) coated NCA, (b)  $\text{Li}_3\text{PO}_4$  powder and (c) pristine NCA under air. The chart of (a) coated NCA exhibited a large decrease in weight at temperatures from 150 to 300 °C. (b)  $\text{Li}_3\text{PO}_4$  powder also exhibited a large decrease in weight at 150–300 °C, although water desorption from the  $\text{Li}_3\text{PO}_4$  powder might occur at temperatures lower than 150 °C. On the other hand, (c) pristine NCA did not exhibit any large change in weight at temperatures up to 400 °C. It could be confirmed that some kind of compounds took leave from the coated layers during the heat treatment of coated NCA samples. The condensation reaction of  $\text{PO}_4^{3-}$  ions on NCA surfaces can be considered the reason for the decrease in weight during the TG-DTA experiments.

XPS spectra of the coated NCA samples were obtained to determine the composition of the coated layers. Fig. 4 shows atomic percentages in sample surfaces (a–h). In Fig. 4, the percentages of oxygen (O), Ni, Li and phosphorus (P) on the NCA

surfaces are shown representatively. Other elements contained on the NCA surface were cobalt, aluminum and carbon. The origin of carbon might be  $\text{Li}_2\text{CO}_3$  formed on the NCA surface. Pristine NCA particle surfaces are covered with the  $\text{Li}_2\text{CO}_3$  layer because  $\text{Li}_2\text{CO}_3$  was formed by reacting the LiOH residue on pristine NCA with carbon dioxide ( $\text{CO}_2$ ) gas under air in the interval of experiments. When compared with pristine NCA, the percentage of nickel on the coated NCAs is higher. The percentages of Li and P decreased in the coated NCAs. The Ni percentages gradually increased with increasing heat treatment temperature. The O and P elements were almost constant. The XPS spectra (Fig. 5) of P in the coated NCA surfaces are characteristic. The XPS spectra for 2p of the coated NCAs shifted to lower binding energy with the increase in heat-treatment temperature. In the case of heat treatment under an air atmosphere, the XPS peak shift for 2p can be observed even at 200 °C. The 2p peak for  $\text{Li}_3\text{PO}_4$  can be observed at 133.2 eV, as shown in Fig. 5.<sup>41</sup> The 2p peak at approximately 130 eV can be assigned to

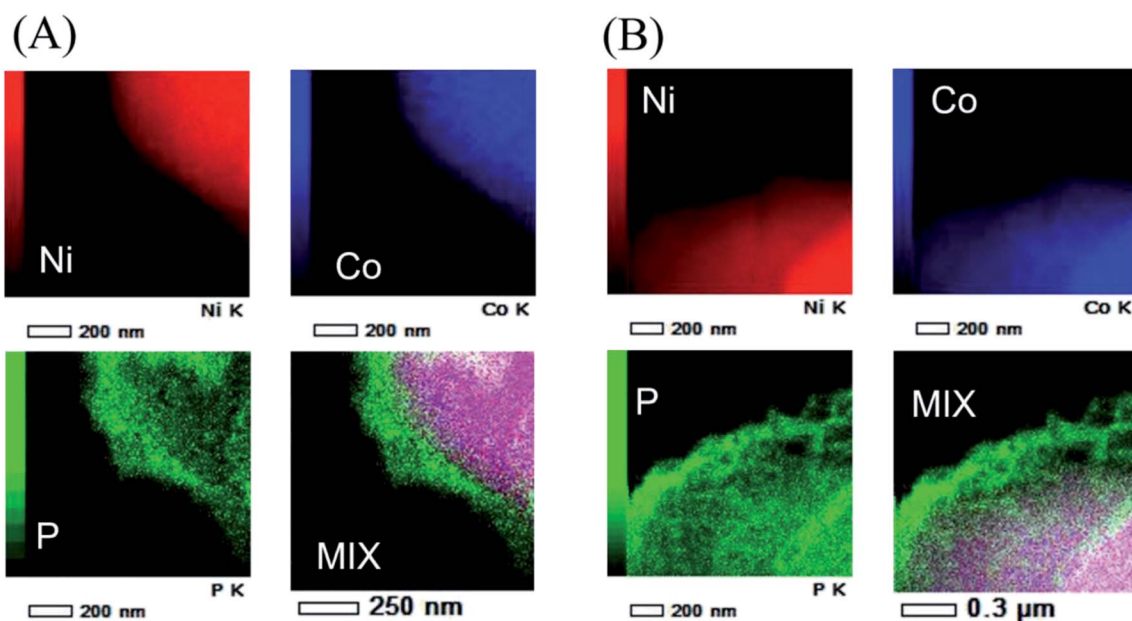


Fig. 3 STEM-EELS mapping of Ni, Co and P elements and their mixed mapping of coated NCA with heat treatment at 400 °C in (A) Ar and (B) air atmospheres.

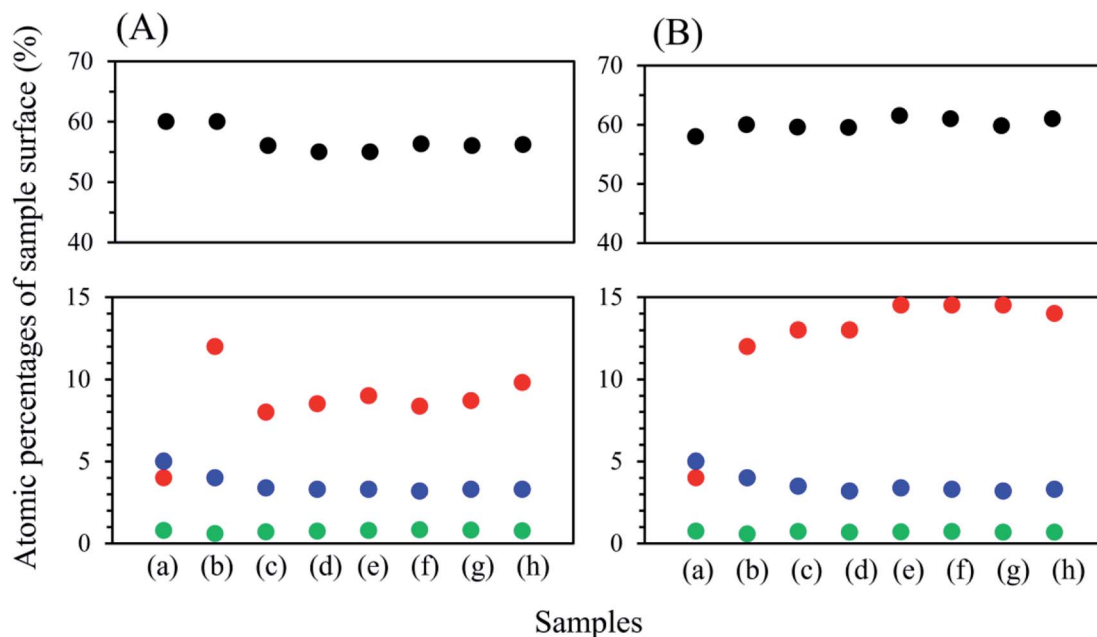


Fig. 4 Atomic percentage on the surface of samples evaluated with XPS. (a) Pristine NCA and (b–h) coated NCA samples. (b)  $\text{Li}_3\text{PO}_4$ -coated NCA samples without heat treatment, (c–h) coated NCA with heat treatment. Temperature of heat treatment: (c) 200, (d) 250, (e) 300, (f) 350, (g) 400 and (h) 450 °C. Atmosphere for heat-treatment: (A) Ar and (B) air. ●: oxygen, ●: nickel, ●: lithium, ●: phosphorus.

one for nickel phosphate ( $\text{Ni}_3(\text{PO}_4)_2$ ).<sup>42</sup> The heat treatment of the coated NCA samples produced  $\text{Ni}_3(\text{PO}_4)_2$  in the coated layers, and  $\text{Li}_3\text{PO}_4$  disappeared from the surface of NCA during the heat treatment. The process with and without heat treatment did not change the oxidation state of Ni on the NCA surfaces.

To identify the crystal structures of the coated layers and NCAs, pXRD patterns of the coated NCA samples were

measured (Fig. 6(A-1) and (B-1)). The pXRD profiles obtained matched that of a layered  $\alpha$ - $\text{NaFeO}_2$ -type structure with the space group  $R\bar{3}m$ ,<sup>43</sup> in which the Na sites are occupied by  $\text{Li}^+$  ions and the Fe sites by transition metal (Ni, Co and Al) ions. The (003) peaks of the coated NCA samples shift to higher angles, and the degree of the (003) peak shift increases with the temperature of the heat treatment (Fig. 6(A-2) and (B-2)),

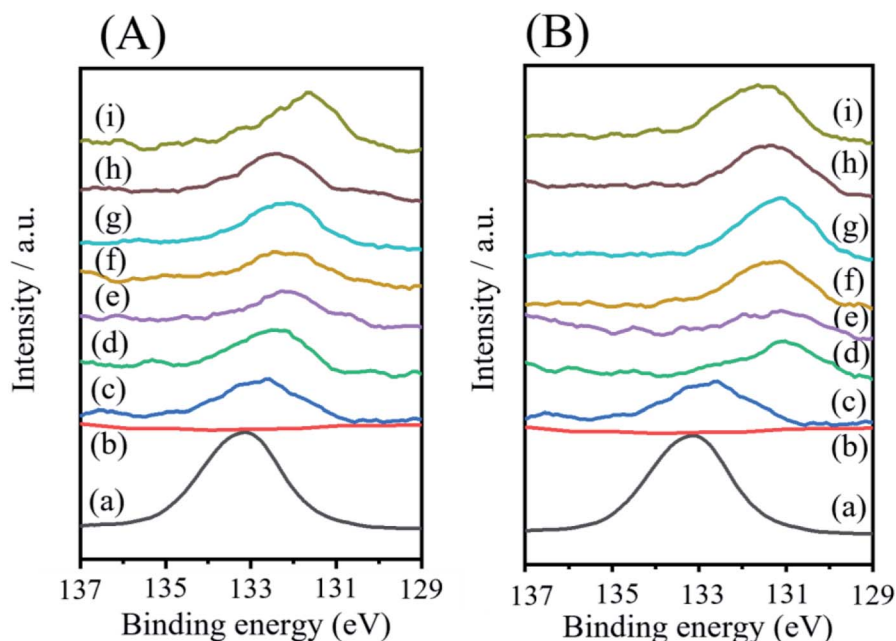


Fig. 5 XPS spectral profiles in the P 2p region of (a)  $\text{Li}_3\text{PO}_4$  powder, (b) pristine NCA and (c–i) coated NCA. Sample (c) was not heat-treated, and samples (d–i) were heat-treated at (d) 200, (e) 250, (f) 300, (g) 350, (h) 400 and (i) 450 °C in (A) Ar and (B) air atmospheres.

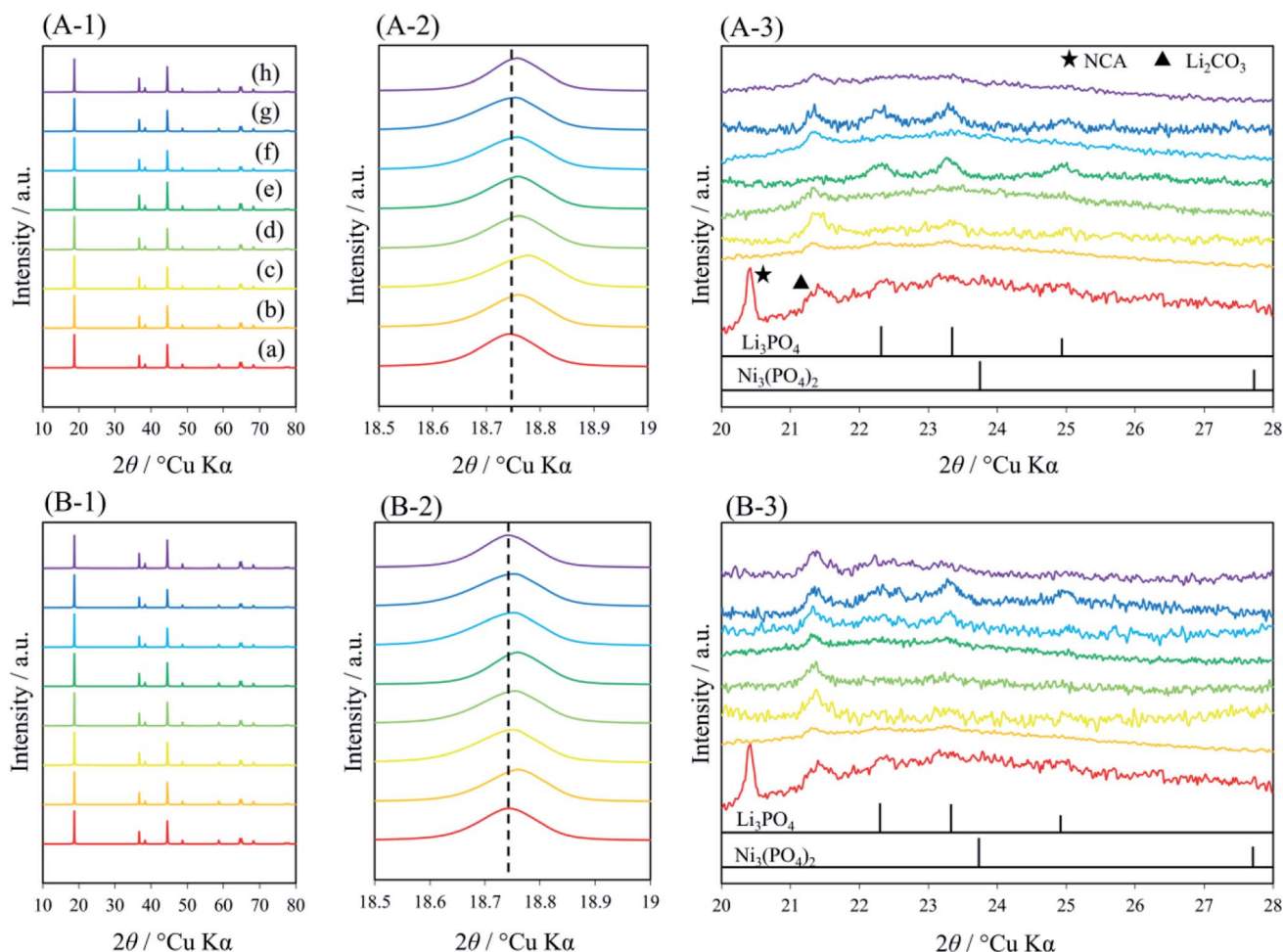


Fig. 6 pXRD patterns of (a) pristine NCA and (b–h) coated NCA with standard peak patterns of  $\text{Li}_3\text{PO}_4$  (JCPDS 83-0339) and  $\text{Ni}_3(\text{PO}_4)_2$  (JCPDS 46-1388). Sample (b) was not heat-treated, and samples (c–h) were heat-treated at (c) 200, (d) 250, (e) 300, (f) 350, (g) 400 and (h) 450 °C in (A) Ar and (B) air atmospheres.

indicating that the coated layers affect the crystal structure of the NCA surface themselves. In addition, the coated NCA samples prepared under an air atmosphere exhibited larger peak shifts than those prepared under an Ar atmosphere. The pXRD peaks corresponding to  $\text{Li}_3\text{PO}_4$  (ref. 44) and  $\text{Li}_2\text{CO}_3$  can be observed in the enlarged pXRD patterns of the samples (Fig. 6(A-3) and (B-3)). However, the peaks for  $\text{Ni}_3(\text{PO}_4)_2$ , which are considered to exist in the coated layers with the XPS results, cannot be observed in the enlarged pXRD patterns. The heat treatment of the coated NCA samples might produce amorphous  $\text{Ni}_3(\text{PO}_4)_2$  on the surface of the coated layer of NCAs.

Taken together with the results of TG-DTA, XPS and pXRD, it can be considered that the formation of the coated layer containing  $\text{Ni}_3(\text{PO}_4)_2$  and  $\text{Li}_3\text{PO}_4$  in the heat treatment occurs, as shown in Fig. 7.  $\text{H}_3\text{PO}_4$  added to the mixture of ethanol/water adsorbs on the surface of NCA and is a source of protons for the exchange of  $\text{Li}^+/\text{H}^+$  (intercalation/deintercalation of  $\text{Li}^+/\text{H}^+$  into/from NCA). Following the intercalation of protons, nickel ions ( $\text{Ni}^{2+}$ ) dissolve, and  $\text{Ni}(\text{OH})_2$  forms on the NCA surfaces. At the same time,  $\text{Li}^+$  deintercalated from the NCA surfaces forms  $\text{LiOH}$  and  $\text{Li}_3\text{PO}_4$  on the NCA surfaces. As mentioned above,

$\text{Li}_3\text{PO}_4$  is formed also in eqn (1). The coated layers containing  $\text{Li}_3\text{PO}_4$ ,  $\text{LiOH}$ ,  $\text{H}_3\text{PO}_4$  and  $\text{Ni}_3(\text{PO}_4)_2$  are very thick on the NCA surfaces. During the heat treatment, the coated layer is dehydrated, and then  $\text{Li}_3\text{PO}_4$  and  $\text{Ni}_3(\text{PO}_4)_2$  are left. The dense coated layers constructed by  $\text{Li}_3\text{PO}_4$  and  $\text{Ni}_3(\text{PO}_4)_2$  have water-stable properties. Based on the XPS results, the dense coated layers consist mainly of  $\text{Ni}_3(\text{PO}_4)_2$ .  $\text{Ni}_3(\text{PO}_4)_2$  does not have a crystal structure in the coated layers. Heat treatment under an air atmosphere enhanced the formation of dense  $\text{Li}_3\text{PO}_4/\text{Ni}_3(\text{PO}_4)_2$ . The reason for the difference between the coated layers prepared with the heat treatments under the Ar and air atmosphere, that is the heat treatment under air atmosphere produce thinner  $\text{Ni}_3(\text{PO}_4)_2$ -rich coat layers, cannot be made clear yet. However, although clear evidence is not obtained, we think that oxygen in air contributes to the formation of thinner coated layers; for example, during heat treatment, oxygen repairs the dissolved oxide surface of NCAs, and then the condensation reaction of  $\text{PO}_3^{4-}$  ions and the formation reaction of  $\text{Ni}_3(\text{PO}_4)_2$  occurs effectively on the repaired NCA surfaces.

Fig. 8 shows the SEM images of (a) pristine NCA particles, (b) uncoated NCA particles and (c–g) coated NCA particles that were

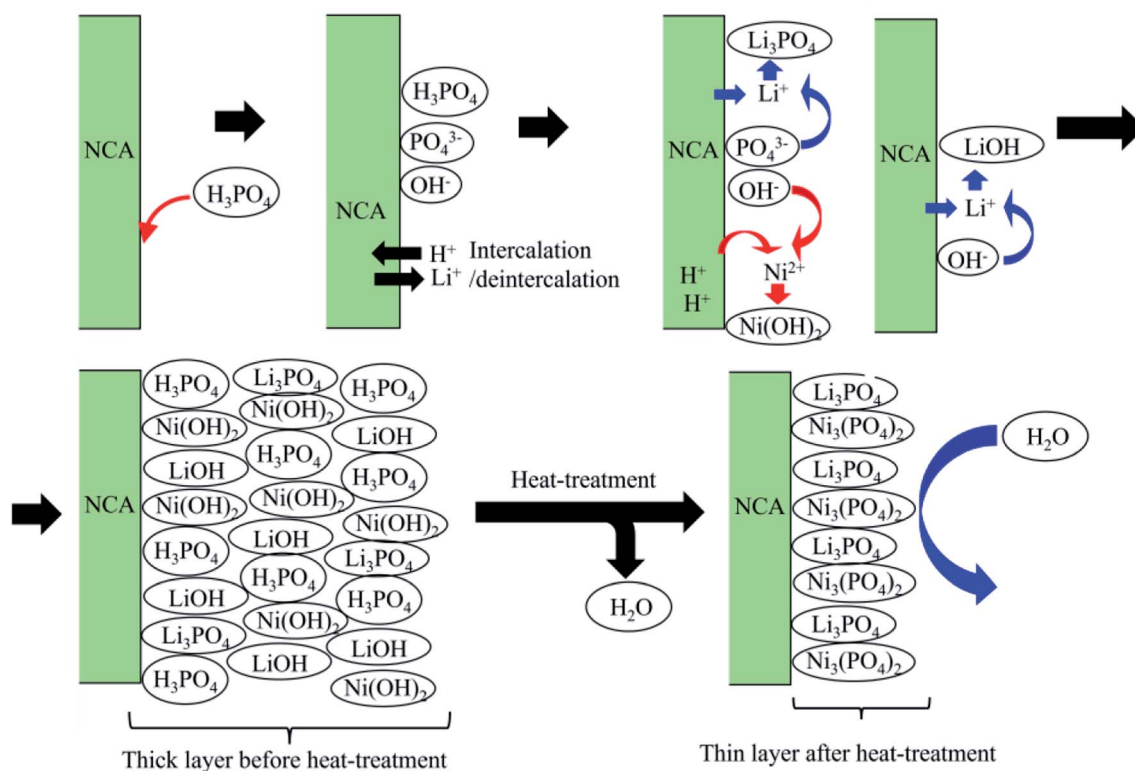


Fig. 7 Schematic description of the formation of the coated layer containing  $\text{Ni}_3(\text{PO}_4)_2$  and  $\text{Li}_3\text{PO}_4$  in the heat treatment.

not (c) or were (d–g) heat-treated at 200 (d, e) and 400 (f, g) °C under Ar (d, f) and air (e, g). Samples (b)–(g) were immersed in water for 1 h to confirm the water stability of the samples before SEM observations. When compared with the SEM image of the pristine NCA sample (a), the uncoated NCA sample that was exposed to water for 1 h was damaged significantly due to the dissolution of the surface into water (b). From the SEM images

of coated NCA samples ((c)–(g)), it was confirmed that the surface roughness of the coated NCA samples increased due to the formation of coating moieties on the NCA surfaces and that the coated NCA samples did not suffer damage from water contact.

Fig. S3† shows the results of the examination of changes in the slurry pH. An aqueous slurry containing CMC and AB

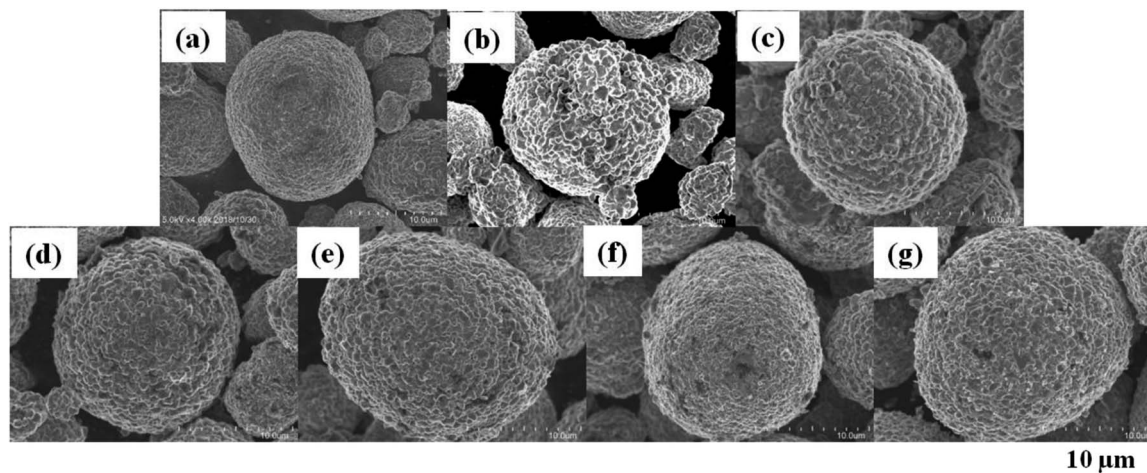


Fig. 8 SEM images of NCA particles. (a) Pristine NCA, (b) uncoated NCA, (c) coated NCA without heat treatment, (d) coated NCA after heat treatment at 200 °C in Ar, (e) coated NCA after heat treatment at 200 °C in air, (f) coated NCA after heat treatment at 400 °C in Ar, and (g) coated NCA after heat treatment at 400 °C in air. SEM images of (b)–(g) samples were obtained after immersion of samples in water for 1 h and drying for 1 h at 130 °C.

without NCA as a blank slurry maintained a pH of approximately 7.5 until 90 min after slurry preparation (a). On the other hand, the pH of the slurry containing uncoated NCA was over 12.5 (b). The coated NCA without and with heat treatment depressed the increase in pH of the slurries after adding the coated NCA to the slurry solutions. Among them, the pH of the coated NCA samples after heat treatment at 350 and 400 °C was lower than that of the other samples. The lowest pH was observed in the coated NCA sample after heat treatment at 400 °C in air. Although an increase in the pH of slurries could be observed, the dissolution of Ni from NCA to the slurry solutions could not be detected in the ICP-MS analysis of the slurry solutions. The reason for the increase in slurry pH even when coated NCA was added to slurry solutions is considered to be due to the exchange of  $H^+$  in  $H_2O$  with  $Li^+$  in  $Li_3PO_4$ , and if Ni ions are dissolved from NCA, Ni ions remain on the NCA surface by forming  $Ni(OH)_2$  and  $Ni_3(PO_4)_2$ . Because the coated layers formed in the 350 and 400 °C heat treatments block water contact with the NCA surface, the exchange reaction of  $H^+/Li^+$  was suppressed among the samples tested. In contrast, the coated layers on NCAs that were heat-treated at 200–300 °C were sparse. Therefore, the exchange reaction of  $H^+/Li^+$  occurred easily, resulting in the relatively high pH of slurry solutions.

### 3.2 Charging/discharging cycle performance tests with coated NCA materials and comparison of them with samples prepared with other preparation methods

Fig. 9 shows the charging/discharging cycle performance obtained with the cathodes prepared from pristine NCA (a, b) and coated NCA samples without (c) and with heat treatment at 200–450 °C (d–i) under Ar (1) and air (2) atmospheres. The cathodes were prepared with PVdF (a) or TRD202A (b–i) binders. In addition, in the case of the TRD202A binder, the slurries containing NCA particles, AB, CMC and TRD202A binder were stored for 1 (A) and 24 (B) h before preparation of the cathodes. The cathode (a) prepared with pristine NCA and PVdF binder exhibited a discharge capacity of 200 mA h  $g^{-1}$  in the first cycle, and the discharge capacity decreased with an increase in the cycle number to 190 mA h  $g^{-1}$  at 20 cycles. The decrease in discharge capacity is an inherent property of pristine NCA. The noncoated NCA cathode (b) prepared with the TRD202A binder exhibited a large decrease in discharge capacity at the first cycle and a large degradation of the discharge capacity with the cycles. The cycle performance of cathodes is in the order follow as

(A-1) Slurry storage 1 h, Ar atmosphere in the heat-treatment. Pristine NCA with PVdF =  $Li_3PO_4$ -coated NCA with heat treatment at 300 °C > 400 °C > 350 °C > 250 °C >  $Li_3PO_4$ -coated NCA without heat treatment > 450 °C > 200 °C.

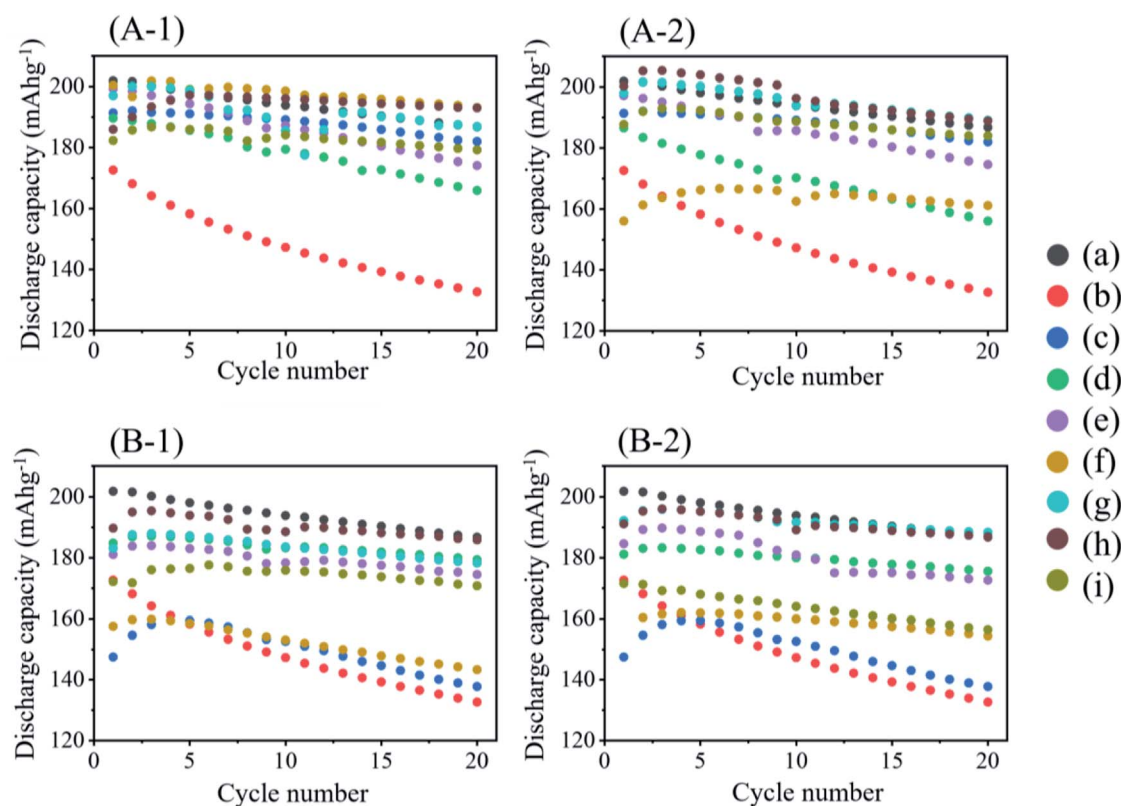


Fig. 9 Plots of discharge capacity vs. charge/discharge cycle number obtained with the NCA cathodes. (a) Pristine NCA cathode prepared with PVdF binder, (b) pristine NCA cathode prepared with TRD202A binder, (c–i) coated NCA cathodes. Sample (c) was not heat-treated, and samples (d–i) were heat-treated at (d) 200, (e) 250, (f) 300, (g) 350, (h) 400 and (i) 450 °C in (1) Ar and (2) air atmospheres. When cathodes were prepared with TRD202A binder, aqueous slurries were stored for (A) 1 and (B) 24 h.



(A-2) Slurry storage 1 h, air atmosphere in the heat treatment. Pristine NCA with PVdF = 400 °C > 350 °C > Li<sub>3</sub>PO<sub>4</sub>-coated NCA without heat treatment = 450 °C > 250 °C > 200 °C > 300 °C.

(B-1) Slurry storage 24 h, Ar atmosphere in the heat-treatment. Pristine NCA with PVdF > 400 °C > 350 °C = 200 °C > 250 °C > 450 °C > 300 °C > Li<sub>3</sub>PO<sub>4</sub>-coated NCA without heat treatment.

(B-2) Slurry storage 24 h, air atmosphere in the heat-treatment. Pristine NCA with PVdF > 400 °C > 350 °C > 250 °C = 200 °C > 450 °C > 300 °C > Li<sub>3</sub>PO<sub>4</sub>-coated NCA without heat treatment.

Although the order of cycle performance among the cathodes examined is not fixed in the cases of (A-1), (A-2), (B-1) and (B-2), the cathodes ((g) and (h)) prepared with coated NCAs treated at 350 and 400 °C exhibited relatively high cathode performance. This trend can be related to one of the pH values in cathode slurries shown in Fig. S3.† Namely, the samples that did not show a large increase in the pH of the slurry can exhibit comparable discharge capacity and cyclability with those observed with cathodes prepared with pristine NCA and PVdF binders. In Fig. 10, the results of coated NCA in this study were compared with coated NCA prepared with ethanol-<sup>35</sup> and water-<sup>37</sup>based slurries. The coated NCA samples were reproduced faithfully with ref. 35 and 37 as samples for comparison. However, when cathodes were prepared with the Li<sub>3</sub>PO<sub>4</sub>-coated NCA samples, all slurries in which the coated NCA samples, AB and CMC were dispersed in water were stored for 1 h before preparation of cathodes to confirm the water stability of the coated NCA samples. The coated NCA sample prepared with ethanol/water-based slurry, which was developed in this study, exhibited the same cathode performance as that of a pristine NCA cathode prepared with PVdF. It means that the formation of (Ni<sub>3</sub>(PO<sub>4</sub>)<sub>2</sub>) and Li<sub>3</sub>PO<sub>4</sub> in the coating layer does not affect the

capacity of NCA cathode. The weight% of (Ni<sub>3</sub>(PO<sub>4</sub>)<sub>2</sub>) and Li<sub>3</sub>PO<sub>4</sub> in the coated NCA is important. However, the weight% of (Ni<sub>3</sub>(PO<sub>4</sub>)<sub>2</sub>) and Li<sub>3</sub>PO<sub>4</sub> in the coated NCA cannot be evaluated because it is very small and the thickness is less than 10 nm as can be expected from TEM image in Fig. 2. When the capacities (mA h g<sup>-1</sup>) of the NCA and non-coated NCA cathodes were evaluated, the weight% of (Ni<sub>3</sub>(PO<sub>4</sub>)<sub>2</sub>) and Li<sub>3</sub>PO<sub>4</sub> was not considered. In the comparison between capacities of the coated and non-coated NCA cathodes in Fig. 10, the difference in the capacities cannot be observed. Therefore, the weight% of (Ni<sub>3</sub>(PO<sub>4</sub>)<sub>2</sub>) and Li<sub>3</sub>PO<sub>4</sub> in the coated NCA is so small. The cathodes prepared with ethanol- and water-based slurries show a decrease in discharge capacity even in the first cycle. In several cycles since the first cycle, the discharge capacity of the cathodes prepared with ethanol- and water-based slurries increased. However, the capacities could not reach one of the cathodes prepared with ethanol/water-based slurry. It can be confirmed that the coated NCA sample examined in this study has the highest water stability.

### 3.3 High rate performance test of coated NCA materials and comparison of them with samples prepared with other preparation methods

The high rate performance of the abovementioned cathodes prepared with ethanol/water-based slurries was examined, and the results were compared with those of TiO<sub>x</sub>-, Li<sub>2</sub>CO<sub>3</sub>- and TiO<sub>x</sub>/Li<sub>2</sub>CO<sub>3</sub>-coated NCA cathodes (Fig. 11). TiO<sub>x</sub>-, Li<sub>2</sub>CO<sub>3</sub>- and TiO<sub>x</sub>/Li<sub>2</sub>CO<sub>3</sub>-coated NCA cathodes were examined in our previous papers.<sup>15,29</sup> These samples have water stability enough to exhibit inherent performance of NCA even after exposing the

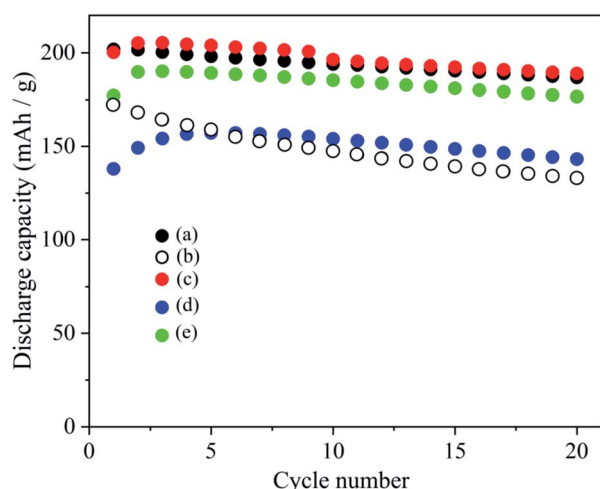


Fig. 10 Plots of discharge capacity vs. charge/discharge cycle number obtained with the NCA cathodes. (a) Pristine NCA cathode prepared with PVdF binder. (b) Pristine NCA cathode prepared with TRD202A binder. Sample (c) was coated NCA prepared in a mixture of water and ethanol. Sample (d) was coated NCA prepared in water. Sample (e) was coated NCA prepared in ethanol. NCA slurries prepared with water/ethanol, water or ethanol were stored for 1 h before preparing the cathodes.

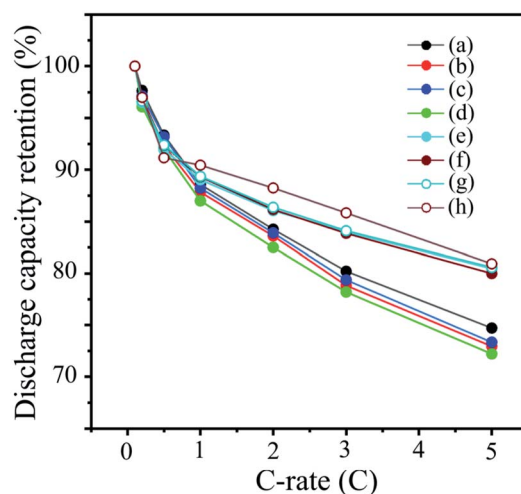


Fig. 11 Plots of discharge capacity retention vs. C-rate obtained with the cathodes prepared from (a) pristine NCA and PVdF binder, (b) TiO<sub>x</sub>/Li<sub>2</sub>CO<sub>3</sub>-, (c) TiO<sub>x</sub>- and (d–h) the coated NCAs. Cathodes (b–h) were prepared with a TRD202A water-based binder. Coated NCA (b) was not heat-treated. The coated NCAs (c–h) were not heat-treated at (e, g) 350 and (f, h) 400 °C in (e, f) Ar and (g, h) air atmospheres. In the calculation of the discharge capacity retention, a discharge capacity of 200 mA h g<sup>-1</sup>, which was observed at the pristine NCA cathode prepared with PVdF binder, was considered 100% capacity retention.

coated NCA particles in water-based slurries for long times. However, the  $\text{TiO}_x$ -,  $\text{Li}_2\text{CO}_3$ - and  $\text{TiO}_x/\text{Li}_2\text{CO}_3$ -coated NCA cathodes exhibited lower rate performance than one of pristine NCA cathodes prepared with PVdF binder because the  $\text{TiO}_x$ -,  $\text{Li}_2\text{CO}_3$ - and  $\text{TiO}_x/\text{Li}_2\text{CO}_3$ -coating layers inhibited  $\text{Li}^+$ -ion transfer through the coating layers for the intercalation/deintercalation processes to/from NCA surfaces. Four cathodes prepared with the coated NCA samples heat-treated at 350 and 400 °C under Ar and air atmospheres clearly showed higher rate performance than one of pristine NCAs prepared with PVdF. The purpose of this study was to confirm that the coated NCA samples heat-treated at 350 and 400 °C under Ar and air atmospheres, which were originally examined in this study, have both water stability and high cathode performance for the first time. The reason for the improvement of rate performance on the coated NCA samples heat-treated at 350 and 400 °C under Ar and air atmosphere might be enhancement of  $\text{Li}^+$ -ion transfer in the coating layers. It has been reported that a coated NCA cathode prepared with PVdF binder exhibited a higher rate performance than an uncoated NCA cathode prepared with PVdF binder.<sup>37,45,46</sup> In addition, the high-rate performance of  $\text{Ni}_3(\text{PO}_4)_2$ -coated NCA cathodes compared with uncoated NCA cathodes prepared with PVdF binders has been reported.<sup>47</sup> Although the composition of the coated layer cannot yet be determined,  $\text{Li}_3\text{PO}_4$  or  $\text{Ni}_3(\text{PO}_4)_2$  layers, which we assumed based on the characterization results of the synthesized samples in this study, could be formed on NCA surfaces to achieve the required water stability and high cycle and rate performance.

## 4 Conclusion

Optimization of the concentration of  $\text{H}_3\text{PO}_4$  added to the slurry for cathode preparation, the ratio of ethanol and water used to prepare the cathode slurry as solvents and the temperature for heat-treatment of coated NCA samples realized water-stable NCA samples, which can be applied to aqueous processes for cathode preparation. Coating layers containing  $\text{Ni}_3(\text{PO}_4)_2$  and  $\text{Li}_3\text{PO}_4$  were formed on NCA surfaces and contributed to the improvement of the water stability of NCA cathode materials. The coating layers could prohibit the NCA surface from damage due to water contact for 24 h. The  $\text{Ni}_3(\text{PO}_4)_2$  and  $\text{Li}_3\text{PO}_4$  species in the coated layers collaborate to improve cathode performance, such as cyclability and high-rate performance.  $\text{Ni}_3(\text{PO}_4)_2$  protects the NCA surface from water contact, and  $\text{Li}_3\text{PO}_4$  enhances the transfer of  $\text{Li}^+$  through the coated layers. In this study, the analysis of coated layers formed on NCA surfaces has not been completed, and the distribution and atomic ratio of  $\text{Ni}_3(\text{PO}_4)_2$  and  $\text{Li}_3\text{PO}_4$  in the coated layers are still unknown. Deep examination of the coated layers and the reasons why the coated layers of  $\text{Ni}_3(\text{PO}_4)_2$  and  $\text{Li}_3\text{PO}_4$  can improve water stability and high-rate performance and why the performance difference between air and Ar treated samples can be observed are in progress.

## Author contribution

T. W. and T. Y. performed charge/discharge test and preparation of coated cathode materials. M. Y and T. G. characterized

the synthesized materials with STEM and EDS. S. K., S. U. and H. L. performed coating treatment of cathode materials. Y. I. and F. M. performed a preparation of bare cathode material and preparation of figures. J. W., T. O. and F. M. wrote the manuscript, summarized the work.

## Conflicts of interest

There are no conflicts to declare.

## Acknowledgements

This work was supported by NIMS microstructural characterization platform as a program of “Nanotechnology Platform” of the Ministry of Education, Culture, Sports, Science and Technology (MEXT), Japan.

## References

- 1 G. Zubi, R. Dufo-López, M. Carvalho and G. Pasaoglu, The lithium-ion battery: state of the art and future perspectives, *Renew. Sustain. Energy Rev.*, 2018, **89**, 292–308.
- 2 M. Broussely and G. Archdale, Li-ion batteries and portable power source prospects for the next 5–10 years, *J. Power Sources*, 2004, **136**, 386–394.
- 3 M. A. Hannan, M. M. Hoque, A. Mohamed and A. Ayob, Review of energy storage systems for electric vehicle applications: Issues and challenges, *Renew. Sustain. Energy Rev.*, 2017, **69**, 771–789.
- 4 F. T. Wagner, B. Lakshmanan and M. F. Mathias, Electrochemistry and the future of the automobile, *J. Phys. Chem. Lett.*, 2010, **1**, 2204–2219.
- 5 J. B. Goodenough and Y. Kim, Challenges for Rechargeable Li Batteries, *Chem. Mater.*, 2010, **22**, 587–603.
- 6 J. M. Tarascan and M. Armand, Issues and challenges facing rechargeable lithium batteries, *Nature*, 2001, **414**, 359–367.
- 7 W. Li, B. Song and A. Manthiram, High-voltage positive electrode materials for lithium-ion batteries, *Chem. Soc. Rev.*, 2017, **46**, 3006–3059.
- 8 J.-L. Shi, R. Qi, X.-D. Zhang, P.-F. Wang, W.-G. Fu, Y.-X. Yin, J. Xu, L.-J. Wan and Y.-G. Guo, High-thermal- and air-stability cathode material with concentration-gradient buffer for Li-ion batteries, *ACS Appl. Mater. Interfaces*, 2017, **9**, 42829–42835.
- 9 K. Liu, Y. Liu, D. Lin, A. Pei and Y. Cui, Materials for lithium-ion battery safety, *Sci. Adv.*, 2018, **4**, eaas9820.
- 10 J. Cabana, B. J. Kwon and L. Hu, Mechanisms of degradation and strategies for the stabilization of cathode–electrolyte interfaces in Li-ion batteries, *Acc. Chem. Res.*, 2018, **51**, 299–308.
- 11 J. Wang, Y. Yamada, K. Sodeyama, E. Watanabe, K. Takada, Y. Tateyama and A. Yamada, Fire-extinguishing organic electrolytes for safe batteries, *Nat. Energy*, 2018, **3**, 22–29.
- 12 W. He, P. Liu, B. Qu, Z. Zheng, H. Zheng, P. Deng, P. Li, S. Li, H. Huang, L. Wang, Q. Xie and D.-L. Peng, Uniform  $\text{Na}^+$  doping-induced defects in Li- and Mn-rich cathodes for

- high-performance lithium-ion batteries, *Adv. Sci.*, 2019, **6**, 1802114.
- 13 T. Liu, S.-X. Zhao, L.-L. Gou, X. Wu and C.-W. Nan, Electrochemical performance of Li-rich cathode material,  $0.3\text{Li}_2\text{MnO}_3\text{-}0.7\text{LiMn}_{1/3}\text{Ni}_{1/3}\text{Co}_{1/3}\text{O}_2$  microspheres with F-doping, *Rare Met.*, 2019, **38**, 189–198.
- 14 W.-W. Li, X.-J. Zhang, J.-J. Si, J. Yang and X.-Y. Sun,  $\text{TiO}_2$ -coated  $\text{LiNi}_{0.9}\text{Co}_{0.08}\text{Al}_{0.02}\text{O}_2$  cathode materials with enhanced cycle performance for Li-ion batteries, *Rare Met.*, 2021, **40**, 1719–1726.
- 15 T. Tanabe, Y. B. Liu, K. Miyamoto, Y. Irii, F. Maki, F. Maki, T. Gunji, S. Kaneko, S. Ugawa, H. Lee, T. Ohsaka and F. Matsumoto, Synthesis of Water-Resistant Thin  $\text{TiO}_x$  Layer-Coated High-Voltage and High-Capacity  $\text{LiNi}_a\text{Co}_b\text{Al}_{1-a-b}\text{O}_2$  ( $a > 0. > 0.85$ ) Cathode and Its Cathode Performance to Apply a Water-Based Hybrid Polymer Binder to Li-Ion Batteries, *Electrochim. Acta*, 2017, **258**, 1348–1355.
- 16 T. Tanabe, T. Gunji, Y. Honma, K. Miyamoto, T. Tsuda, Y. Mochizuki, S. Kaneko, S. Ugawa, H. Lee, T. Ohsaka and F. Matsumoto, Preparation of Water-Resistant Surface Coated High-Voltage  $\text{LiNi}_{0.5}\text{Mn}_{1.5}\text{O}_4$  Cathode and Its Cathode Performance to Apply a Water-Based Hybrid Polymer Binder to Li-Ion Batteries, *Electrochim. Acta*, 2017, **224**, 429–438.
- 17 D. Bresser, D. Buchholz, A. Moretti, A. Varzi and S. Passerini, Alternative binders for sustainable electrochemical energy storage – the transition to aqueous electrode processing and bio-derived polymers, *Energy Environ. Sci.*, 2018, **11**, 3096–3127.
- 18 A. Iturrondobeitia, A. Kvasha, J.-M. Lopez del Amo, J. F. Colin, D. Sotta, I. Urdampilleta and M. Casas-Cabanas, A comparative study of aqueous and organic processed  $\text{Li}_{1.2}\text{Ni}_{0.2}\text{Mn}_{0.6}\text{O}_2$  Li-rich cathode materials for advanced lithium-ion batteries, *Electrochim. Acta*, 2017, **247**, 420–425.
- 19 D. L. Wood III, J. Li and C. Daniel, Prospects for reducing the processing cost of lithium ion batteries, *J. Power Sources*, 2016, **275**, 234–242.
- 20 W. Liu, P. Oh, X. Liu, M.-J. Lee, W. Cho, S. Chae, Y. Kim and J. Cho, Nickel-rich layered lithium transition-metal oxide for high-energy lithium-ion batteries, *Angew. Chem., Int. Ed.*, 2015, **54**, 4440–4457.
- 21 K. Hoang and M. Johannes, Defect physics and chemistry in layered mixed transition metal oxide cathode materials: (Ni,Co,Mn) vs (Ni,Co,Al), *Chem. Mater.*, 2016, **28**, 1325–1334.
- 22 S.-T. Myung, F. Maglia, K.-J. Park, C. S. Yoon, P. Lamp, S.-J. Kim and Y.-K. Sun, Nickel-rich layered cathode materials for automotive lithium-ion batteries: achievements and perspectives, *ACS Energy Lett.*, 2017, **2**, 196–223.
- 23 Y. Makimura, T. Sasaki, T. Nonaka, Y. F. Nishimura, T. Uyama, C. Okuda, Y. Itou and Y. Takeuchi, Factors affecting cycling life of  $\text{LiNi}_{0.8}\text{Co}_{0.15}\text{Al}_{0.05}\text{O}_2$  for lithium-ion batteries, *J. Mater. Chem. A*, 2016, **4**, 8350–8358.
- 24 S. Hwang, S. M. Kim, S.-M. Bak, B.-W. Cho, K. Y. Chung, J. Y. Lee, W. Chang and E. A. Stach, Investigating local degradation and thermal stability of charged nickel-based cathode materials through real-time electron microscopy, *ACS Appl. Mater. Interfaces*, 2014, **6**, 15140–15147.
- 25 W. B. Hawley, A. Parejiya, Y. Bai, H. M. Meyer III, D. L. Wood III and J. Li, Lithium and transition metal dissolution due to aqueous processing in lithium-ion battery cathode active materials, *J. Power Sources*, 2020, **466**, 228315.
- 26 L. Hartmann, D. Pritzl, H. Beyer and H. A. Gasteiger, Evidence for  $\text{Li}^+/\text{H}^+$  exchange during ambient storage of Ni-rich cathode active materials, *J. Electrochem. Soc.*, 2021, **168**, 070507.
- 27 I. Hamam, N. Zhang, A. Liu, M. B. Johnson and J. R. Dahn, Study of the reactions between Ni-rich positive electrode materials and aqueous solutions and their relation to the failure of Li-ion cells, *J. Electrochem. Soc.*, 2020, **167**, 130521.
- 28 M. Hofmann, M. Kapuschinski, U. Guntow and G. A. Giffin, Implications of aqueous processing for high energy density cathode materials: part I. Ni-rich layered oxides, *J. Electrochem. Soc.*, 2020, **167**, 140512.
- 29 T. Watanabe, K. Hirai, F. Ando, S. Kurosumi, S. Ugawa, H. Lee, Y. Irii, F. Maki, T. Gunji, J. Wu, T. Ohsaka and F. Matsumoto, Surface double coating of a  $\text{LiNi}_a\text{Co}_b\text{Al}_{1-a-b}\text{O}_2$  ( $a > 0.85$ ) cathode with  $\text{TiO}_x$  and  $\text{Li}_2\text{CO}_3$  to apply a water-based hybrid polymer binder to Li-ion batteries, *RSC Adv.*, 2020, **10**, 13642–13654.
- 30 K. Kimura, K. Onishi, T. Sakamoto, K. Asami and M. Yanagida, Achievement of the high-capacity retention rate for the  $\text{Li}[\text{Ni}_{0.8}\text{Co}_{0.15}\text{Al}_{0.05}]\text{O}_2$  (NCA) cathode containing an aqueous binder with  $\text{CO}_2$  gas treatment using the cavitation effect (CTCE), *J. Electrochem. Soc.*, 2019, **166**, A5313–A5317.
- 31 W. B. Hawley, H. M. Meyer III and J. Li, Enabling aqueous processing for  $\text{LiNi}_{0.80}\text{Co}_{0.15}\text{Al}_{0.05}\text{O}_2$  (NCA)-based lithium-ion battery cathodes using polyacrylic acid, *Electrochim. Acta*, 2021, **380**, 138203.
- 32 W. Bauer, F. A. Çetinel, M. Müller and U. Kaufmann, Effects of pH control by acid addition at the aqueous processing of cathodes for lithium ion batteries, *Electrochim. Acta*, 2019, **317**, 112–119.
- 33 K. Soeda, M. Yamagata and M. Ishikawa, Alginate acid as a new aqueous slurry-based binder for cathode materials of LIB, *ECS Trans.*, 2015, **64**, 13–22.
- 34 M. Hofmann, F. Nagler, M. Kapuschinski, U. Guntow and G. A. Giffin, Surface modification of  $\text{LiNi}_{0.8}\text{Co}_{0.15}\text{Al}_{0.05}\text{O}_2$  particles via  $\text{Li}_3\text{PO}_4$  coating to enable aqueous electrode processing, *ChemSusChem*, 2020, **13**, 5962–5971.
- 35 M. Hofmann, F. Nagler, U. Guntow, G. SEXTL and G. A. Giffin, Long-term cycling performance of aqueous processed Ni-rich  $\text{LiNi}_{0.8}\text{Co}_{0.15}\text{Al}_{0.05}\text{O}_2$  cathodes, *J. Electrochem. Soc.*, 2021, **168**, 060511.
- 36 X. Bian, Q. Fu, X. Bie, P. Yang, H. Qiu, Q. Pang, G. Chen, F. Du and Y. Wei, Improved electrochemical performance and thermal stability of Li-excess  $\text{Li}_{1.18}\text{Co}_{0.15}\text{Ni}_{0.15}\text{Mn}_{0.52}\text{O}_2$  cathode material by  $\text{Li}_3\text{PO}_4$  surface coating, *Electrochim. Acta*, 2015, **174**, 875–884.
- 37 S. Chen, T. He, Y. Su, Y. Lu, L. Bao, L. Chen, Q. Zhang, J. Wang, R. Chen and F. Wu, Ni-rich  $\text{LiNi}_{0.8}\text{Co}_{0.1}\text{Mn}_{0.1}\text{O}_2$  oxide coated by dual-conductive layers as high

- performance cathode material for lithium-ion batteries, *ACS Appl. Mater. Interfaces*, 2017, **9**, 29732–29743.
- 38 W. Zhang, L. Liang, F. Zhao, Y. Liu, L. Hou and C. Yuan, Ni-rich  $\text{LiNi}_{0.8}\text{Co}_{0.1}\text{Mn}_{0.1}\text{O}_2$  coated with Li-ion conductive  $\text{Li}_3\text{PO}_4$  as competitive cathodes for high-energy-density lithium ion batteries, *Electrochim. Acta*, 2020, **340**, 135871.
- 39 Q. Gan, N. Qin, Z. Wang, Z. Li, Y. Zhu, Y. Li, S. Gu, H. Yuan, W. Luo, L. Lu, Z. Xu and Z. Lu, Revealing Mechanism of  $\text{Li}_3\text{PO}_4$  Coating Suppressed Surface Oxygen Release for Commercial Ni-Rich Layered Cathodes, *ACS Appl. Energy Mater.*, 2020, **3**, 7445–7455.
- 40 A. T. Appapillai, A. N. Mansour, J. Cho and Y. Shao-Horn, Microstructure of  $\text{LiCoO}_2$  with and without “ $\text{AlPO}_4$ ” nanoparticle coating: combined STEM and XPS studies, *Chem. Mater.*, 2007, **19**, 5748–5757.
- 41 J. Chang, Q. Lv, G. Li, J. Ge, C. Liu and W. Xing, Core-shell structured  $\text{Ni}_{12}\text{P}_5/\text{Ni}_3(\text{PO}_4)_2$  hollow spheres as difunctional and efficient electrocatalysts for overall water electrolysis, *Appl. Catal., B*, 2017, **204**, 486–496.
- 42 M. Bichon, D. Sotta, N. Dupré, E. D. Vito, A. Boulineau, W. Porcher and B. Lestriez, Study of immersion of  $\text{LiNi}_{0.5}\text{Mn}_{0.3}\text{Co}_{0.2}\text{O}_2$  material in water for aqueous processing of positive electrode for Li-ion batteries, *ACS Appl. Mater. Interfaces*, 2019, **11**, 18331–18341.
- 43 J. Xie, J. F. M. Oudenhoven, P.-P. R. M. L. Harks, D. Li and P. H. L. Notten, Chemical vapor deposition of lithium phosphate thin-films for 3D all-solid-state Li-ion batteries, *J. Electrochem. Soc.*, 2015, **162**(3), A249–A254.
- 44 M. A. Al-Omair, M. M. Khalaf, A. H. Touny, H. Elsayy and M. M. Saleh, Antimicrobial activities of mesoporous nickel phosphate synthesized with low-temperature method, *Microchem. J.*, 2019, **145**, 113–118.
- 45 M. Wang, R. Zhang, Y. Gong, Y. Su, D. Xiang, L. Chen, Y. Chen, M. Luo and M. Chu, Improved electrochemical performance of the  $\text{LiNi}_{0.8}\text{Co}_{0.1}\text{Mn}_{0.1}\text{O}_2$  material with lithium-ion conductor coating for lithium-ion batteries, *Solid State Ionics*, 2017, **312**, 53–60.
- 46 Y. Lee, J. Lee, K. Y. Lee, J. Mun, J. K. Lee and W. Choi, Facile formation of a  $\text{Li}_3\text{PO}_4$  coating layer during the synthesis of a lithium-rich layered oxide for high-capacity lithium-ion batteries, *J. Power Sources*, 2016, **315**, 284–293.
- 47 D.-J. Lee, B. Scrosati and Y.-K. Sun,  $\text{Ni}_3(\text{PO}_4)_2$ -coated  $\text{Li}[\text{Ni}_{0.8}\text{Co}_{0.15}\text{Al}_{0.05}]\text{O}_2$  lithium battery electrode with improved cycling performance at 55 °C, *J. Power Sources*, 2011, **196**, 7742–7746.